Influences of asymmetric quantum wells on electron-phonon interactions



2001 J. Phys.: Condens. Matter 13 6489

(http://iopscience.iop.org/0953-8984/13/30/304)

INSTITUTE OF PHYSICS PUBLISHING JOURNAL OF PHYSICS: CONDENSED MATTER

J. Phys.: Condens. Matter **13** (2001) 6489–6498 PII: S0953-8984(01)24014-4

# Influences of asymmetric quantum wells on electron–phonon interactions

**V N Stavrou**[1], **M Babiker and C R Bennett**

Physics Department, University of Essex, Colchester CO4 3SQ, UK

E-mail: vasilios.stavrou@dlr.de

Received 18 April 2001, in final form 1 June 2001
Published 13 July 2001
Online at stacks.iop.org/JPhysCM/13/6489

**Abstract**

We calculate the electron capture rates for electrons at the bottom of the first subband above a CdSe quantum well surrounded by ZnSe and ZnS barrier layers. The electron capture mechanism is defined as the transition of an electron at the bottom of the first subband above the quantum well into all possible subbands within the quantum well by the emission of optical phonons, described here by the dielectric continuum model. The asymmetry of the structure influences the shape of the interface modes which must be taken into account together with the confined modes in each material. It is found that the capture rates depend on the width of the quantum well. At regular intervals of well width sharp peaks appear which correspond to *electron and phonon resonances*. Furthermore the asymmetry of the structure does not allow the capture rates to drop to very small values unlike the symmetric quantum well (e.g. GaN/AlN).

## 1. Introduction

In the last few years, there has been considerable worldwide experimental research effort directed towards the study of electronic and optical devices made of II–VI semiconductor compounds (for example ZnSe and alloys ZnCdSe and ZnSSe) [1, 2] and nitrides (GaN) [3]. The strong thrust of this work has been motivated by the prospect of producing the next generation of quantum well lasers designed to operate at short wavelengths, approximately in the blue/green region of the electromagnetic spectrum [2, 3].

The rate of electron capture by a quantum well is an important factor when designing quantum well lasers. Earlier theoretical work on the capture rates was based on either a well defined initial state [4, 5] or averaging contributions from the possible initial states over a suitable distribution function [6–8]. In this paper we assume that the electrons are injected

[1] Permanent address: Institute of Technical Physics, DLR, Pfaffenwaldring 38–40, University of Stuttgart, D-70569 Stuttgart, Germany.

  

optically into the bottom of the first subband above the well and are then captured into the well. The capture mechanism is assumed to be by the emission of phonons which are described by dielectric continuum (DC) model [9–11]. The DC model has been used in the past to calculate the capture rates in the case of a symmetric AlN/GaN structure [5]. The aim of this paper is, on the one hand, to investigate the influence of the asymmetric structure on the interface phonons (IP) modes and, on the other hand, to investigate the dependence of capture rates on well width in asymmetric quantum wells.

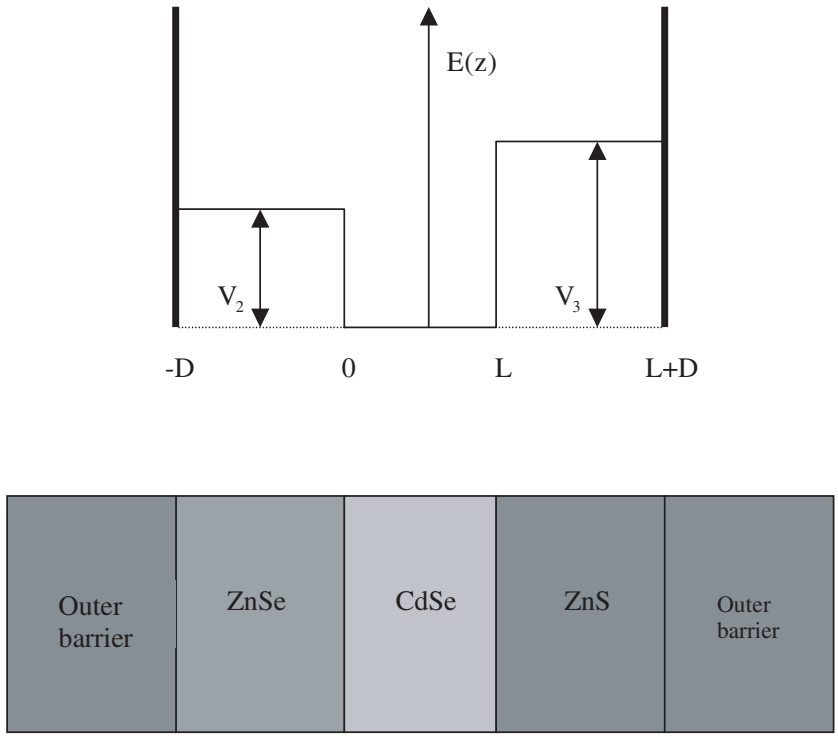


**Figure 1.** An asymmetric structure using the materials ZnSe, CdSe and ZnS.

## 2. Electron states

Let us consider the heterostructure as defined in figure 1. The quantum well is made of CdSe surrounded by ZnSe and ZnS barrier layers and the whole structure is sandwiched between two infinite outer barriers. The role of the outer barriers is to produce a discrete energy spectrum above the well and a zero electric potential for the phonons. The electron wavefunction $\psi(\boldsymbol{r})$ allowed by this heterostructure with an energy eigenvalue $E$ is given by

$$\psi(\boldsymbol{k}_\parallel, z) = \frac{1}{2\pi} \mathrm{e}^{\mathrm{i}\boldsymbol{k}_\parallel \cdot \boldsymbol{r}_\parallel} f(z) \tag{1}$$

where we have written $\boldsymbol{r} = (\boldsymbol{r}_\parallel, z)$ and $\boldsymbol{k}_\parallel$ is a two-dimensional wavevector along the interface planes.

It is convenient to introduce the wavevectors for a given $E$ and $\boldsymbol{k}_\parallel$ as

$$k_i^2 = \begin{cases} \dfrac{2m_2^*(E-V_2)}{\hbar^2} - k_\parallel^2 & \text{with } i=2,\ -D<z<0 \\ \dfrac{2m_1^*E}{\hbar^2} - k_\parallel^2 & \text{with } i=1,\ 0<z<L \\ \dfrac{2m_3^*(E-V_3)}{\hbar^2} - k_\parallel^2 & \text{with } i=3,\ L<z<L+D. \end{cases} \tag{2}$$

The boundary conditions at the inner interfaces are the continuity of the wavefunction $\Psi$ and the derivative $1/m_i^*(\partial\Psi/\partial z)$ (where $m_i^*$ is the effective mass in material $i$). At the outer interfaces the boundary condition is the vanishing of $\Psi$.

The solution $f(z)$ for electron energy $E(\boldsymbol{k}_\parallel = 0) < V_2$ conforming with these boundary conditions is found to be

$$f(z) = A_1 \begin{cases} \dfrac{\sinh(k_2(z+D))}{\sinh(k_2D)} & -D<z<0 \\ \cos(k_1z) + a\coth(k_2D)\sin(k_1z) & 0<z<L \\ -\dfrac{\cos(k_1L) + a\coth(k_2D)\sin(k_1L)}{\sinh(k_3D)}\sinh[k_3(z-(D+L))] & L<z<L+D \end{cases} \tag{3}$$

where $A_1$ is a coefficient to be determined by normalization and $a = k_2m_1^*/k_1m_2^*$. In this case where $E(\boldsymbol{k}_\parallel = 0) < V_2$, $k_2$ and $k_3$ are purely imaginary and this forces $f(z)$ to decay exponentially away from the inner interfaces.

In the case where $V_2 < E(\boldsymbol{k}_\parallel = 0) < V_3$, the general solution takes the form

$$f(z) = A_1' \begin{cases} \dfrac{\sin(k_2(z+D))}{\sin(k_2D)} & -D<z<0 \\ \cos(k_1z) + a\cot(k_2D)\sin(k_1z) & 0<z<L \\ -\dfrac{\cos(k_1L) + a\cot(k_2D)\sin(k_1L)}{\sinh(k_3D)}\sinh[k_3(z-(D+L))] & L<z<L+D \end{cases} \tag{4}$$

where $A_1'$ is another coefficient to be determined by normalization. In this case the wavevectors $k_1$ and $k_2$ are real and $k_3$ is purely imaginary.

As well as the wavefunctions in (3) and (4), the application of the above mentioned boundary conditions leads to the dispersion relation for the initial electron states for $V_2 < E(\boldsymbol{k}_\parallel = 0) < V_3$ in the form

$$\tan(k_1L) = \frac{b + a\cot(k_2D)\tanh(k_3D)}{\tanh(k_3D) - ab\cot(k_2D)} \tag{5}$$

and for the final electron states, where $E(\boldsymbol{k}_\parallel = 0) < V_2$, we have the dispersion relation

$$\tan(k_1L) = \frac{b + a\coth(k_2D)\tanh(k_3D)}{\tanh(k_3D) - ab\coth(k_2D)} \tag{6}$$

where $b = k_3m_1^*/k_1m_3^*$.

The variations of the electronic subband minima with the well width are shown in figure 2 where the barrier width is fixed at the value $D = 200$ Å and the parameters of the materials that have been used in our calculations (table 1) are mentioned in [12]. This figure clearly shows the well widths $L_c$, $L_1$, $L_2$, $L_3$, ... at which the electronic state just above the quantum well enters the quantum well.

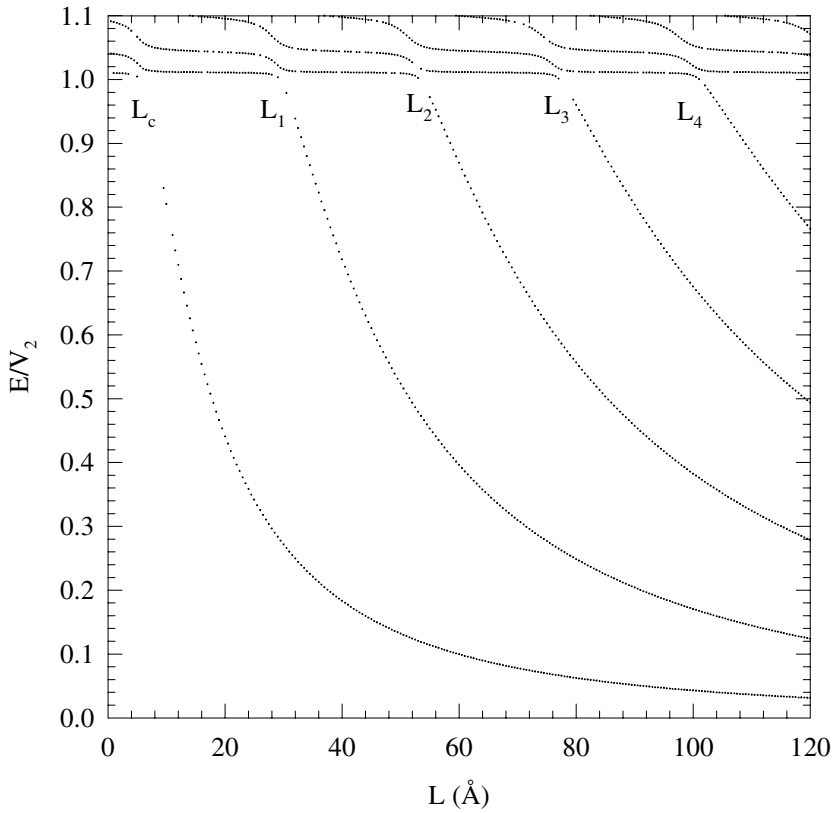


**Figure 2.** Variation of the subband minima with well width for the asymmetric quantum well ZnSe/CdSe/ZnS with barrier width $D = 200$ Å.

We can now plot the modulus square of the wavefunction for the various subbands against position $z$ in the layer structure as shown in figure 3. This plot presents the electronic probability distributions for the first excited electron state in which the subband energy minimum is above $V_2$ and below $V_3$ ($V_2 < E(\boldsymbol{k}_\parallel = 0) < V_3$). The barrier width was chosen as $D = 200$ Å and the well width as $L = 50$ Å, $L = 53$ Å, $L = 54$ Å and $L = 55$ Å. Note that in these figures the electron distribution for the state just above the quantum well is predominantly in the barrier (ZnSe) region. Even at the well width where the electron resonance occurs ($L = 53$ Å) there is a substantial barrier distribution of this state. This is clearly due to the finite value of $D$ and the behaviour is very similar to the barrier state that was found to exist above the well in a superlattice [13].

## 3. DC phonons

The DC model is distinguished by two types of optical modes, namely the confined and interface modes. These modes satisfy the electromagnetic boundary conditions that at any planar interface between two different polar materials the tangential component of the electric field vector and the normal component of the electric displacement field vector both be continuous. The normalization of these types of mode follows a similar procedure as in the symmetric quantum well case [11, 14] will lead to the normalized phonon potentials.

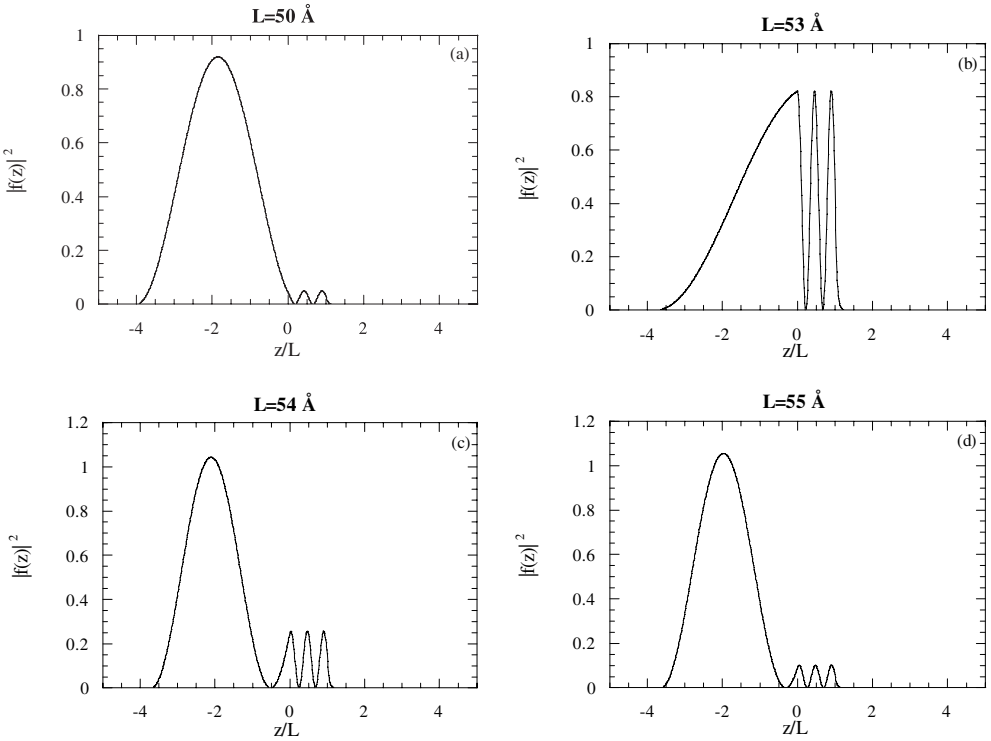


**Figure 3.** Spatial distribution of the first excited electronic state outside the asymmetric quantum well ZnSe/CdSe/ZnS for a quantum well width: (a) $L = 50$ Å; (b) $L = 53$ Å; (c) $L = 54$ Å and (d) $L = 55$ Å with barrier width $D = 200$ Å.

### *3.1. Confined modes*

The confined modes have zero potential at the interface and their frequency always corresponds to the LO phonon of the confining material. In the case of an asymmetric structure three different confined modes exist with interaction Hamiltonians given by

$$\hat{H}_I^{Conf}(\boldsymbol{r}, z, t) = \begin{cases} \displaystyle\sum_n \int [C^{Conf2}(n, \boldsymbol{q}_\parallel, z) \exp[\mathrm{i}(\boldsymbol{q}_\parallel \cdot \boldsymbol{r} - \omega_{L2} t)] \hat{a}_{n,\boldsymbol{q}_\parallel} + HC]\, \mathrm{d}^2 \boldsymbol{q}_\parallel \\ \qquad -D < z < 0 \\ \displaystyle\sum_m \int [C^{Conf1}(m, \boldsymbol{q}_\parallel, z) \exp[\mathrm{i}(\boldsymbol{q}_\parallel \cdot \boldsymbol{r} - \omega_{L1} t)] \hat{a}_{m,\boldsymbol{q}_\parallel} + HC]\, \mathrm{d}^2 \boldsymbol{q}_\parallel \\ \qquad 0 < z < L \\ \displaystyle\sum_p \int [C^{Conf3}(p, \boldsymbol{q}_\parallel, z) \exp[\mathrm{i}(\boldsymbol{q}_\parallel \cdot \boldsymbol{r} - \omega_{L3} t)] \hat{a}_{p,\boldsymbol{q}_\parallel} + HC]\, \mathrm{d}^2 \boldsymbol{q}_\parallel \\ \qquad L < z < L + D \end{cases} \tag{7}$$

where $\hat{a}_{\boldsymbol{q}_\parallel}$ ($\hat{a}^\dagger_{\boldsymbol{q}_\parallel}$) is the annihilation (creation) operator satisfying the usual commutator relationships with wavevector $\boldsymbol{q} = (\boldsymbol{q}_\parallel, q_z)$, HC stands for Hermitian conjugate. The quantization procedure is considered in such a manner that the field Hamiltonian (7) reduces

**Table 1.** Material parameters used in the calculations.

| | CdSe | ZnSe | ZnS |
|---|---|---|---|
| $m_e$ ($m_0$) | 0.13 | 0.17 | 0.28 |
| $E_{gap}$ (eV) | 1.74 | 2.58 | 3.80 |
| $\omega_L$ (meV) | 26.36 | 30.45 | 43.56 |
| $\omega_T$ (meV) | 20.67 | 25.62 | 34.90 |

to the canonical form. Thus, the coefficients $C_m^{Conf1}$, $C_n^{Conf2}$ and $C_p^{Conf3}$ are given by

$$C^{Conf1}(n, \boldsymbol{q}_\parallel, z) = \left[\frac{e^2\hbar^2\omega_{L1}}{2\varepsilon_0\pi^2\xi_1(\omega_{L1})}\frac{L}{\boldsymbol{q}_\parallel^2 L^2 + n^2\pi^2}\right]^{1/2} \sin\left(\frac{n\pi z}{L}\right) \tag{8}$$

$$C^{Conf2}(m, \boldsymbol{q}_\parallel, z) = \left[\frac{e^2\hbar^2\omega_{L2}}{2\varepsilon_0\pi^2\xi_2(\omega_{L2})}\frac{L}{\boldsymbol{q}_\parallel^2 L^2 + m^2\pi^2(L/D)}\right]^{1/2} \sin\left(\frac{m\pi z}{L}\right) \tag{9}$$

$$C^{Conf3}(p, \boldsymbol{q}_\parallel, z) = \left[\frac{e^2\hbar^2\omega_{L3}}{2\varepsilon_0\pi^2\xi_3(\omega_{L3})}\frac{L}{\boldsymbol{q}_\parallel^2 L^2 + p^2\pi^2(L/D)}\right]^{1/2} \sin\left(\frac{p\pi(z-L)}{D}\right) \tag{10}$$

with $\varepsilon_i(\omega)$ the dielectric function for material $i$ and $\xi_i(\omega) = \omega\partial\varepsilon_i(\omega)/\partial\omega$.

### *3.2. IP modes*

The interface modes have potential maxima at the inner interfaces and vanish at the outer interfaces. The Hamiltonian of the interface modes is given by [11, 14]

$$\hat{H}_I^{IP}(\boldsymbol{r}, z, t) = \sum_j \int [C_j^{IP}(\boldsymbol{q}_\parallel, z)\exp[\mathrm{i}(\boldsymbol{q}_\parallel \cdot \boldsymbol{r} - \omega_{\boldsymbol{q}_\parallel, j}t)]\hat{a}_{j,\boldsymbol{q}_\parallel} + HC]\,\mathrm{d}^2\boldsymbol{q}_\parallel \tag{11}$$

where $j$ denotes the interface branch and following the same quantization procedure as in the case of confined modes the coefficient $C_j^{IP}(\boldsymbol{q}_\parallel, z)$ is defined as

$$C_j^{IP}(\boldsymbol{q}_\parallel, z) = \sqrt{\frac{e^2\hbar\omega_{\boldsymbol{q}_\parallel, j}}{(2\pi)^2\varepsilon_0\{\xi_1(\omega_{\boldsymbol{q}_\parallel, j})\lambda_1 + \xi_2(\omega_{\boldsymbol{q}_\parallel, j})\lambda_2 + \xi_3(\omega_{\boldsymbol{q}_\parallel, j})E^2\lambda_3\}}} \times \begin{cases} \sinh(\boldsymbol{q}_\parallel(z+D)) & -D < z < 0 \\ A\cosh(\boldsymbol{q}_\parallel z) + B\sinh(\boldsymbol{q}_\parallel z) & 0 < z < L \\ E\sinh(\boldsymbol{q}_\parallel(z-(D+L))) & L < z < L + D. \end{cases} \tag{12}$$

In (12) the unknown parameters are defined by

$$\lambda_1 = \boldsymbol{q}_\parallel\left(AB(\cosh(2\boldsymbol{q}_\parallel L) - 1) + (A^2 + B^2)\frac{\sinh(2\boldsymbol{q}_\parallel L)}{2}\right) \tag{13}$$

$$\lambda_2 = \lambda_3 = \frac{\boldsymbol{q}_\parallel}{2}\sinh(2\boldsymbol{q}_\parallel D) \tag{14}$$

$$A = \sinh(\boldsymbol{q}_\parallel D) \tag{15}$$

$$B = \frac{\varepsilon_2\cosh(\boldsymbol{q}_\parallel D)}{\varepsilon_1} \tag{16}$$

$$E = -\frac{(\varepsilon_2/\varepsilon_1)\sinh(\boldsymbol{q}_\parallel L)\cosh(\boldsymbol{q}_\parallel D) + \sinh(\boldsymbol{q}_\parallel D)\cosh(\boldsymbol{q}_\parallel L)}{\sinh(\boldsymbol{q}_\parallel D)}. \tag{17}$$

The IP mode relation in the asymmetric structure is obtained as

$$\frac{\varepsilon_1(\varepsilon_2+\varepsilon_3)}{\varepsilon_1^2\tanh(q_\parallel D)+\varepsilon_2\varepsilon_3\coth(q_\parallel D)} = -\tanh(q_\parallel L). \tag{18}$$

The metal barriers contain a large number of free electrons forming a free electron gas which exhibits plasma properties. The plasmons in the metallic barriers have not been taken into account because the plasmon modes, for large $D$, correspond to high or low energies (large or small frequencies) [15] and they do not contribute to the scattering rates as a result of the conservation of energy in the equation (19).

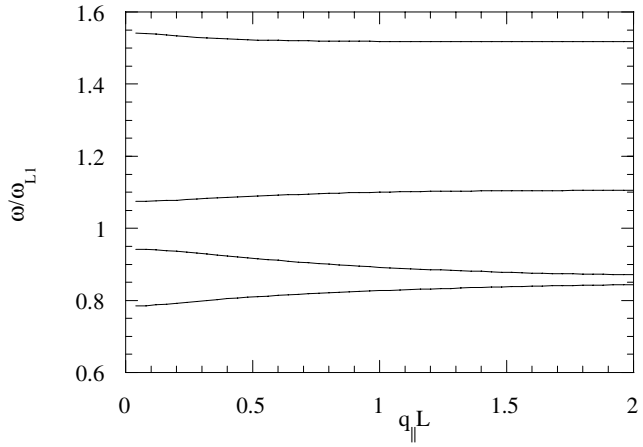


**Figure 4.** The interface phonon branches for the asymmetric quantum well ZnSe/CdSe/ZnS with barrier width $D = 200$ Å and well width $L = 150$ Å.

The dispersion curves of the interface phonon modes in an asymmetric quantum well are presented in figure 4. It is clear from figure 4 that the two top branches correspond to the *reststrahl* bands of ZnSe and ZnS. Finally, it should be noted that the IP modes can not be separated into symmetric and antisymmetric modes, as in the case of symmetric quantum wells systems, because of the explicit asymmetry of the heterostructure.

## 4. Capture rates

We have defined the capture rate as the transition rate of electrons from the bottom of the first subband ($i$) above the well to all possible states within subbands in the quantum well ($n$). The capture rate is given by Fermi's golden rule as

$$\Gamma = \frac{2\pi}{\hbar}\sum_{all\ modes}\sum_{\substack{all\ final\\ states\ n}}|\langle\Psi_n|\hat{H}_I|\Psi_i\rangle|^2\delta\left(\frac{\hbar^2 q_\parallel^2}{2m_1^*}+\hbar\omega_{q_\parallel}-\Delta E_{i,n}\right). \tag{19}$$

It is convenient to present capture rates in terms of the characteristic rate $\Gamma_0$ for bulk CdSe which is given by

$$\Gamma_0 = \frac{e^2}{4\pi\varepsilon_0\hbar}\left(\frac{1}{\varepsilon_{\infty 1}}-\frac{1}{\varepsilon_{s1}}\right)\left(\frac{2m_1^*\omega_{L1}}{\hbar}\right)^{1/2} = 4.25\times 10^{13}\ \mathrm{s}^{-1}.$$

The effects of changing the well width $L$ in the ZnSe/CdSe/ZnS quantum well structure on the electron capture rate are shown in figure 5 where the barrier width is fixed at $D = 200$ Å.

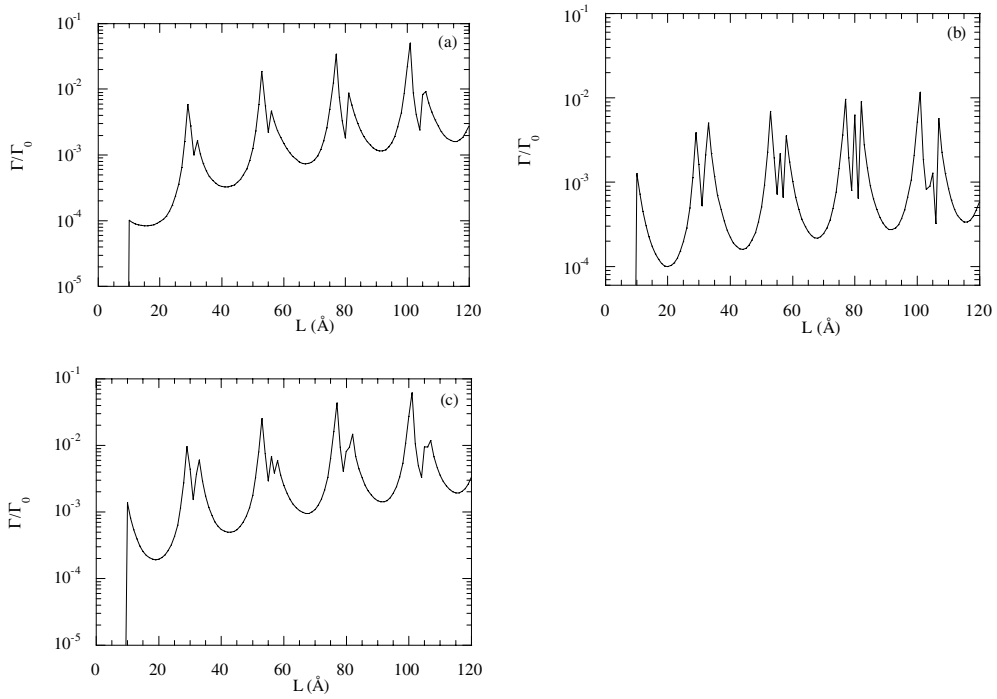


**Figure 5.** Illustration of: (a) the contribution of the confined modes to the capture rates; (b) the contribution of the interface phonon modes to the capture rates; and (c) the total transition rate for the electron capture against the well width in the quantum well ZnSe/CdSe/ZnS with barrier width $D = 200$ Å.

Figure 5(a) presents the contributions to the transition rate from the confined modes, figure 5(b) displays the corresponding contribution from the interface phonon modes and figure 5(c) shows the total capture rates. These results exhibit interesting features which we now discuss.

First the graphs exhibit clear and pronounced peaks at approximately regular intervals. Second, the peak height increases with increasing well width. It can be seen that the peaks are positioned in the regions of well width values $L_1, L_2, L_3, \ldots$ where the initial electronic state, just above the well, enters the quantum well (see figure 2). The probability distributions (for $L = 50, 53, 54, 55$ Å) of this state are shown in figure 3. Clearly as we approach the resonance point $L \approx 53$ Å from below, the probability distribution becomes more concentrated in the well and therefore the matrix element is enhanced. This is the origin of the resonance near $L_2$. Above $L_2$ we switch to a new initial state above the well. This state is mainly in the barrier, hence the reduction after the resonance. The state which has just entered the well would not contribute initially, since the energy separation from the new initial state would be smaller than a typical LO energy. The small peaks on the right shoulder of the resonance are explainable as follows. As the state that has just entered the well moves down in energy with increasing $L$, its separation from the new initial state gradually approaches the phonon energy for one of the allowed branches. This state begins to contribute to the capture process. However, further increase in $L$ leads to smaller contributions until the next resonance point at $L = L_3$ is approached. The procedure is repeated in the next interval and so on.

The decrease of the height of the resonances of the capture rate with decreasing well width is consistent with observation. In experiments [16, 17] for a GaAs/AlAs quantum well

the intensity of recombination radiation emitted by a quantum well system was observed to decrease with decreasing well width. This effect was explained by the suggestion that the narrow quantum wells cease to capture the non-equilibrium electrons effectively generated at energies above the well which have been injected either electrically or optically. Except for experiments involving varying the well width, the resonances of the capture rates could also be observed by changing the initial electron energy by applying a gate voltage. To the best of the authors' knowledge such experiments on carrier capture in the case of asymmetric quantum wells have not been reported.

In the present case the well width difference between the electron resonance and the following phonon resonance is very close and the capture rates do not drop to minimum values. This is in contradiction with the symmetric quantum wells where the antiresonances (lowest capture rates) are very small and stay longer until the appearance of the next phonon resonance [5]. The explicit asymmetry of the structure is responsible for this feature which influences the wavefunctions and the phonon modes.

## 5. Comments and conclusions

The main purpose of the work described in this paper was to examine the influences of an asymmetric heterostructure on the interface modes and the capture rates. As mentioned in the introduction these materials are important because of their potential for green/blue lasers. In this work we have examined the electron–phonon interactions in an asymmetric quantum well made of these materials. For this asymmetric quantum well we have developed the analytical theory of electron capture and calculated numerically the capture rate for electron transitions from the state just above the quantum well to all possible states inside. Transitions are mediated by phonons which are described by the DC model and contributions from all channels have been taken into account. The IP modes have been found that are strongly dependent on the asymmetric heterostructure which is of crucial importance for the capture rates. We have seen that the variation of the capture rate with the well width exhibits some interesting features. First there are resonances which occur near values of the well widths at which the initial state transforms from an unbound state to a bound state within the well. This corresponds to an electron resonance. In the vicinity of this value of $L$ the matrix element becomes large and so does the capture rate. The second feature of the results is that the capture rate maxima increase with increasing well width. This feature is consistent with early experiments on recombination radiation in a quantum well [17]. Comparison with the capture rates for symmetric quantum wells shows that the asymmetric systems do not allow the scattering rates to drop to very small values. This is because of the dependence of the wavefunctions and the DC phonons on the explicit asymmetry of the system.

## Acknowledgment

The authors would like to thank Professor Brian Ridley for useful discussions.

## References

[1] Agrawal G 1995 *Semiconductor Lasers, Past, Present and Future* (New York: AIP)
[2] Akera I 1996 *III-Vs Rev.* **9** 66
Meredith W 1996 *III-Vs Rev.* **9** 56
[3] Fasol G and Nakamura S 2000 *The Blue Laser Diode GaN Based Emitters and Lasers* (Berlin: Springer)
[4] Kozyrev S V and Shik A Ya 1985 *Sov. Phys.–Semicond.* **19** 1025

[5] Stavrou V N, Bennett C R, Babiker M, Zakhleniuk N A and Ridley B K 1998 *Phys. Low-Dim. Struct.* **1/2** 23
Stavrou V N 2000 *J. Phys.: Condens. Matter* **12** 10 535
Stavrou V N, Bennett C R, Al-Dossary O M M and Babiker M 2001 *Phys. Rev.* B **63** 205 304
[6] Brum J A and Bastard G 1986 *Phys. Rev.* B **33** 1420
[7] Yassievich N, Schmalz K and Beer M 1994 *Semicond. Sci. Technol.* **9** 1763
[8] Mansour N S, Kim K W and Littlejohn M A 1995 *J. Appl. Phys.* **77** 2834
[9] Fuchs R and Kliewer K L 1965 *Phys. Rev.* A **140** 2076
[10] Kliewer K L and Fuchs R 1966 *Phys. Rev.* **144** 495
[11] Mori N and Ando T 1989 *Phys. Rev.* B **40** 6175
[12] Jeon H, Ding J, Patterson W and Nurmikko A V 1991 *Appl. Phys. Lett.* **59** 3619
Ferry D K 1991 *Semiconductor* (New York: Macmillan)
Pankove J I 1975 *Optical Processes in Semiconductors* (New York: Dover)
[13] Jaros M and Wong K B 1984 *J. Phys. C: Solid State Phys.* **17** L765
[14] Ridley B K 1997 *Electrons and Phonons in Semiconductor Multilayers* (Cambridge: Cambridge University Press)
[15] Constantinou N C 1993 *Phys. Rev.* B **49** 11 931
Stavrou V N 1999 *PhD Thesis* University of Essex
[16] Holonyak N Jr, Kolbas R M, Dupuis R D and Dapkus P D 1980 *IEEE J. Quantum Electron.* **16** 170
[17] Shichijo H, Kolbas P D, Holonyak N Jr, Dupuis R D and Dapkus 1978 *Solid State Commun.* **27** 1029